Aerosol Science and Technology
Publication details, including instructions for authors and subscription information:
http://www.tandfonline.com/loi/uast20

Population Balance-Monte Carlo Simulation for Gas-to-Particle Synthesis of Nanoparticles

Xiaoming Hao [a] , Haibo Zhao [a] , Zuwei Xu [a] & Chuguang Zheng [a]
[a] State Key Laboratory of Coal Combustion , Huazhong University of Science and Technology , Wuhan , China
Accepted author version posted online: 23 Jul 2013.Published online: 08 Aug 2013.

To cite this article: Xiaoming Hao , Haibo Zhao , Zuwei Xu & Chuguang Zheng (2013) Population Balance-Monte Carlo Simulation for Gas-to-Particle Synthesis of Nanoparticles, Aerosol Science and Technology, 47:10, 1125-1133, DOI: 10.1080/02786826.2013.823642

To link to this article: http://dx.doi.org/10.1080/02786826.2013.823642

Aerosol Science and Technology, 47:1125–1133, 2013

ISSN: 0278-6826 print / 1521-7388 online
DOI: 10.1080/02786826.2013.823642

Population Balance-Monte Carlo Simulation for Gas-to-Particle Synthesis of Nanoparticles

Xiaoming Hao, Haibo Zhao, Zuwei Xu, and Chuguang Zheng
State Key Laboratory of Coal Combustion, Huazhong University of Science and Technology, Wuhan, China

The process simulation of nanoparticle synthesis via the gas-phase method is essential to understanding the detailed dynamic evolution of nanoparticles within a very short time period under high temperature. The task is, however, very challengeable up to now as the conversion of the gaseous precursor to the end-use nanoparticle is a complex physicochemical process involving nucleation of the particulate phase, agglomeration between particles and sintering under industrial production conditions. In this article, we extended the differentially weighted Monte Carlo method for population balance to simulate the dynamic evolution of titania (TiO_2) nanoparticles synthesized by gas-to-particle conversion in a single aerosol reactor, considering simultaneous nucleation, agglomeration, and sintering. The simulated size distribution of TiO_2 agglomerate and primary particles produced by the thermal decomposition of titanium tetraisoproxide agreed well with the experimental data. In the simulation, the fast population balance-Monte Carlo method was utilized to accelerate the process simulation on a desktop PC. Results were obtained up to 178 times faster than that of a normal Monte Carlo method. The inhomogeneous internal structure of primary particles was considered through solving population balance of polydisperse primary particles within agglomerate. It was found the polydisperse model could predict the primary particle size distribution better. Simulation results revealed a complex competition relation among nucleation, agglomeration and sintering.

[Supplementary materials are available for this article. Go to the publisher's online edition of *Aerosol Science and Technology* to view the free supplementary files.]

Received 27 March 2013; accepted 21 June 2013.
The authors were supported by the National Natural Science Foundation of China (51276077, 51021065), Program for New Century Excellent Talents in University (NCET-10-0395), National Key Basic Research and Development Program (2010CB227004), and State Key Laboratory of Multiphase Complex Systems (MPCS-2011-D-02).
Address correspondence to Haibo Zhao, State Key Laboratory of Coal Combustion, Huazhong University of Science and Technology, Luoyu Road 1037, Wuhan 430074, China. E-mail: klinsmannzhb@163.com

1. INTRODUCTION

Nanoparticles synthesis via aerosol route has recently attracted the growing interests of the scientific and industrial communities because it can produce high-purity nanoparticles with specially tailored chemical and physical property, e.g., hybrid component and high specific surface area (SSA), which can be used to produce ceramics, catalysts, pigments, electric, and optical materials (Seto et al. 1997). In the gas-to-particle synthesis route (aerosol processes), particles are built from molecules (by chemical reaction/nucleation) all the way up to the desired size (by condensation, agglomeration, and sintering) (Pratsinis and Vemury 1996; Bandyopadhyaya et al. 2004). Typically in aerosol processes (Nakaso et al. 2001), highly concentrated nanosized nuclei grown from gas monomers by nucleation and surface reaction undergo rapid Brownian agglomeration. At a high temperature, the resultant nanoparticles may fully coalesce into dense spheres almost instantaneously, as the agglomeration rate is far smaller than the sintering rate. As the aerosol reactor cools down, the sintering rate may be far smaller than the agglomeration rate, leading to fractal-like agglomerates consisting of a large number of primary particles (PPs). Gas-phase nucleation, agglomeration, sintering compete in synthesis processes, and affect the size distributions of agglomerates and primary particles. Simulating these phenomena involved helps us better understand the detailed dynamic evolution of nanoparticles within a very short time period (usually less than several seconds) and having an inhomogeneous temperature history, and therefore provides guidance to control property of product particles. Population balance modeling (PBM) is the most effective tool for the process simulation of nanoparticle dynamics, where size and surface area are two key internal variables of particles that should be tracked during the dynamic evolution (Tsantilis et al. 2002).

Deterministic methods for PBM (Hounslow et al. 1988; Kruis et al. 1993; Xiong and Pratsinis 1993; Rosner and Pyykönen 2002; Muhlenweg et al. 2002; Fox 2006) are capable of describing the time (or axial-direction) evolution of nanoparticle volume and surface area. These methods aim at the direct solutions of the following bivariate population balance equation

(PBE), which mathematically formulates the nanoparticle dynamics including nucleation, agglomeration, and sintering:

$$\frac{\partial n(v,a,t)}{\partial t} = \left\{k(t)\, C_{\mathrm{pre}} N_{\mathrm{A}} \delta(v_0,v)\, \delta(a_0,a)\right\}_{\mathrm{nucl}} + \left\{ \begin{array}{l} \frac{1}{2}\int_{v_0}^{v}\int_{a_0}^{a} \beta(v', v-v'; a', a-a'; t) n(v', a', t) \\ \quad \times n(v-v', a-a', t)\mathrm{d}v'\mathrm{d}a' - n(v,a,t)\int_{v_0}^{\infty}\int_{a_0}^{\infty} \\ \quad \times \beta(v', v; a', a; t) n(v', a', t)\mathrm{d}v'\mathrm{d}a' \end{array} \right\}_{\mathrm{agg}} - \left\{ \frac{\partial}{\partial a}\left[\frac{(a-a_{\mathrm{final}})}{\tau_{\mathrm{s}}(v,a)} n(v,a,t)\right]\right\}_{\mathrm{sin}}, \quad [1]$$

where $n(v,a,t)$ is the number density function at time t such that $n(v,a,t)\mathrm{d}v\mathrm{d}a$ represents the number concentration of particles in the volume range v to $v + \mathrm{d}v$ and the surface area range a to $a+\mathrm{d}a$; $k(t)$ is the gas-phase reaction rate, C_{pre} is the mole concentration of gas precursors, N_{A} is the Avogadro's number; $\beta(v',v;a',a;t)$ is the agglomeration rate coefficient (i.e., agglomeration kernel) between one particle of state (v',a') and another particle of state (v,a); $\tau_{\mathrm{s}}(v,a)$ is the characteristic sintering time of one particle of state (v,a), a_{final} is the surface area of the sphere after complete coalescence.

Deterministic methods for PBM have been widely used to gain dynamic evolution of agglomerate and primary particle size distribution. However, the numerical solution of the bivariate PBE poses a number of difficulties due to the double integral and nonlinear behavior of the equation. More unfortunately, these deterministic methods are at a disadvantage of modeling more than two internal variables (e.g., the fractal structure, chemical component, charge). In fact, these functional properties of nanoparticles cannot be characterized by commonly used volume and surface area. In contrast to deterministic integration of the PBE, the population balance-Monte Carlo (PB-MC) method directly simulates the dynamic evolution of a finite sample of the particle population. The advantage of PB-MC methods lies in their simplicity and, more importantly, in their stochastic and discrete nature that adapt itself naturally to nucleation, agglomeration, and sintering (Rosner and Yu 2001; Morgan et al. 2005). Furthermore, the discrete nature of the particles used to represent the system is very useful for multivariate population balances, i.e., containing other particle properties than particle size alone.

The PB-MC methods have been used by several groups to research simultaneous agglomeration and sintering. Rosner and Yu (2001) explored MC-based simulations for agglomeration and sintering, integrated with finite-rate coalescence in the asymptotic limit that characteristic sintering time is much shorter compared with the characteristic agglomeration time. Tandon and Rosner (1999) obtained the self-preserving joint distribution function (with respect to both particle size and surface area) of populations of coagulating fractal agglomerates in the continuum regime, simultaneously undergoing finite-rate restructuring. Kostoglou and Konstandopoulos (2001) studied the evolutions of agglomerate size and fractal dimension during Brownian agglomeration. These researchers usually prefer the constant-number method (Smith and Matsoukas 1998) because the PB-MC method is capable of maintaining a constant number of simulation particles by the appropriate time-tracking procedure. These PB-MC methods, which directly describe the dynamic evolution of internal variables (e.g., size and surface area) of each simulation particle (it represents a certain number of real particles having similar state with the simulation particle), belong to the variant of the direct simulation algorithm or traditional direct simulation Monte Carlo method. In contrast to direct simulation algorithm, the mass flow algorithm uses one stochastic particle to represent mass concentration rather than number concentration of real particles. Morgan et al. (2005) proposed the mass flow algorithm for modeling agglomeration, sintering, nucleation, and surface growth in preparation process of SiO_2 or TiO_2 nanoparticles. Compared with traditional direct simulation algorithm, the mass flow algorithm is more effective and simple, however, at the cost of complicated algorithms and less accuracy in number concentration (Goodson and Kraft 2004).

With respect to gas-to-particle synthesis of nanoparticles via plug-flow aerosol reactors, some experimental measurements and numerical results are available. Seto et al. (1995) studied the sintering characteristics of TiO_2 agglomerates by testing TiO_2 agglomerates produced by thermal decomposition or hydrolysis of titanium tetraisopropoxide (TTIP). They evaluated several characteristic sintering time models, and found that the simulation results are very sensitive to the sintering model. Seto et al. (1997) further measured and simulated (using two-dimensional sectional method) the change in size distributions of agglomerates (like TiO_2 and SiO_2) and primary particles. They found that the sintering of agglomerates occurs at temperatures corresponding to 50–100% of the bulk melting points of the particle material. Nakaso et al. (2001) extended their experimental measurements and population balance modeling to an integral reactor where nucleation, agglomeration, and sintering take place simultaneously. They modeled the growth of both agglomerates and primary particles by two-dimensional discrete-sectional method (DS), considering effect of temperature on the size distribution of TiO_2 nanoparticle product. Park and Rogak (2003) used a one-dimensional model for agglomeration, gradual sintering, condensational obliteration, and diffusional wall deposition in the same aerosol reactor. In their model particles smaller than the "melting diameter" were assumed to sinter instantly while bigger particles did not sinter at all. All these models show significant discrepancy with experimental results, which was attributed to the effect of diffusional wall deposition, precursor reaction rate, condensation, and non-effective characteristic sintering time model. Tsantilis and Pratsinis (2004) found ranges of surface reaction rates lead to narrower size distribution. Nakaso et al. (2003) studied the effect of chemical reaction rate on the size and morphology, and obtained an effective gas-phase reaction rate. Effective characteristic

sintering time equations of SiO_2/TiO_2 were proposed by several groups (Tsantilis et al. 2001; Buesser et al. 2011; Shekar et al. 2012).

This article aims at the process simulation of gas-to-particle-synthesis of nanoparticles using the direct simulation algorithm. The PB-MC method will be very powerful for general simulation of the processes, where more than two internal variables are required to understand more details involved in the synthesis processes. To our best knowledge, very limited literatures are available on PB-MC methods for nanoparticle synthesis starting from the gas phase directly (i.e., considering simultaneous nucleation, agglomeration, and sintering). It is partly ascribed to several drawbacks of popular PB-MC methods. The first drawback relates to the greater CPU time required as compared to (discrete-) sectional models and methods of moments. For example, the normal PB-MC costs nearly a week if no acceleration action is adopted when the simulation particle number is only 1000. The second drawback is the statistical noise inherent to MC methods. Sufficient simulation particles (usually, more than 1000) and several repeated simulations with random number using different seeds are required to fatigue against the statistical noise. What's more, the available PB-MC methods usually track equally weighted simulation particles, which directly leads to an insufficient number of simulation particles in those sections of the size spectrum where the density is low, such as at the two edges of nanoparticle size distribution, and then a great deal of statistical noise for particles in those regions. We have recently proposed a differentially weighted Monte Carlo (DWMC) method for particle coagulation in monvariate (Zhao et al. 2009), multivariate (Zhao et al. 2010, 2011), or multi-dimensioanl (Zhao and Zheng 2013) population balance. The method constructs a new jump Markov process based on a new coagulation rule for two differentially weighted simulation particles, and restricts simulation particle number in each size interval within prescribed bounds during simulation. The DWMC efficiently reduces statistical noise, and has the remarkable advantage of being able to track the size distribution over the full size spectrum (Zhao et al. 2009). In this study, we extended the DWMC method to a single reactor and described simultaneous nucleation, agglomeration, and sintering involved in nanoparticle dynamics in real processes.

2. MODELS

The present simulation is for synthesis process of nanoparticles (TiO_2) produced from thermal decomposition (Equation (2)) of titanium tetraisoproxide (TTIP). The formation rate of TiO_2 nuclei is given by Equation (3) (Okuyama et al. 1990).

$$\mathrm{TTIP} \rightarrow \mathrm{TiO_2} + 4\mathrm{C_3H_6} + 2\mathrm{H_2O}, \quad [2]$$

$$\left[\frac{\partial N(v_0, a_0, t)}{\partial t}\right]_{\mathrm{nucl}} = kC_{\mathrm{pre}}N_{\mathrm{A}} \quad \text{with } k = 3.96 \times 10^5 \times \exp(-8.48 \times 10^3/T), \mathrm{s}^{-1}, \quad [3]$$

where $N(v_0,a_0,t)$ is the number concentration of TiO_2 nuclei (they are considered as spherical particles), C_{pre} represents the mole concentration of precursor (mol/m^3), k is the rate of thermal decomposition (s^{-1}), and N_{A} is Avogadro's number (6.02×10^{23}/mol).

In this article, the Brownian agglomeration kernel in transition regime ($1 < Kn < 50$, $Kn = 2\lambda/d$ with λ the mean free path of the surrounding gas and d the particle diameter) is employed. An approximate kernel valid for the transition regime, which is harmonic mean of the slip flow kernel (β_{sf}) and the free molecular kernel (β_{fm}) (Kazakov and Frenklach 1998; Otto et al. 1999; Patterson et al. 2006), is used

$$\beta_{\mathrm{tr}} = \frac{\beta_{\mathrm{sf}} \cdot \beta_{\mathrm{fm}}}{\beta_{\mathrm{sf}} + \beta_{\mathrm{fm}}}, \quad [4]$$

with respect to sintering, the surface area of agglomerate toward its final area will change with rate of $1/\tau_{\mathrm{s}}$. The characteristic sintering time τ_{s} based on surface diffusion mechanism (Kobata et al. 1991) is:

$$\tau_{\mathrm{s}}(d_{\mathrm{pp}}, T) = 7.44 \times 10^{16} d_{\mathrm{pp}}^4 T \exp\left(\frac{258 \times 10^3}{RT}\right), \mathrm{s}, \quad [5]$$

where d_{pp} is the diameter of primary particle in an agglomerate (m), R is gas constant (J mol^{-1} K^{-1}). The diameter of agglomerate is calculated as (Seto et al. 1997)

$$d_{\mathrm{m}} \approx d_{\mathrm{s}} = \sqrt{\frac{a_{\mathrm{m}}}{\pi}}, \quad [6]$$

where a_{m} is its surface area (m^2), d_{m} and d_{s} are the mobility diameter (m) and the surface area equivalent diameter (m) of an agglomerate.

3. NUMERICAL SIMULATIONS

The gas-to-particle synthesis process is dominated by the interaction of gas-phase nucleation, agglomeration, and sintering. We extended the differentially weighted Monte Carlo (DWMC) method to simulate this process. First, a fast version of the DWMC method was proposed to accelerate greatly simulation of two-particle event (agglomeration here). The constant-number scheme was introduced to keep simulation particle number constant, in case the nucleation event will increase sharply the number of simulation particles especially in the initial stage. In order to reduce cost, the sintering and agglomeration were uncoupled based on the finite-rate sintering idea. With respect to sintering, two models for the size distribution of primary particles (PP) within agglomerates: the monodispersed PP model and the polydispersed PP model (Heine and Pratsinis 2007), were adopted, respectively, and compared with each other. Finally, a comprehensive DWMC was constructed for the process simulation of real aerosol processes.

3.1. Agglomeration and the Fast DWMC Method

In the DWMC, the weight of a simulation particle i, w_i, means that the simulation particle i represents w_i real particles having the same or similar internal variables (i.e., size, area) as i. In order to capture the details of nanoparticle dynamics, the following internal variables of simulation particles are directly tracked: statistical weight w, the volume (or mass) v, the surface area a, the mobility diameter d_m, the diameter of primary particles in an agglomerate d_{pp}, the number of primary particles in an agglomerate N_{pp}. In the monodisperse PP model, it is assumed that primary particles in an agglomerate are same spherical ones; while in the polydisperse PP model (Heine and Pratsinis 2007), it is assumed that an agglomerate consists of PPs with different size, and the representative size and number density of each section of PP distribution are tracked directly.

The agglomeration rule presented in our previous publication (Zhao et al. 2009) is used here, which can be found in the online supplemental information. The interacting particle pairs of an agglomeration event are selected with probability $\beta'_{ij}/\sum_i \sum_{j,j\neq i} \beta'_{ij}$. Either the cumulative probabilities method or the acceptance-rejection (AR) method can be adopted to determine the coagulated pairs in the time-driven mode. In this article, the AR method is highlighted because it may improve computational efficiency in some cases (e.g., with narrow size spectrum) or for some MC methods (e.g., the fast-DWMC presented below). It is worth noting that, even though the maximum of the normalized agglomeration kernel over all possible pairs is overestimated, the AR method can still describe the Markov process exactly but less efficiently.

Noting that the normal-DWMC methods need double looping over all simulation particles to obtain the agglomeration rate of a simulation particle, the waiting time, and the maximum agglomeration kernel, even though the smart bookkeeping technology (which actually requires a regional double looping) is used. This is why the computational cost is as high as $O(N_{st}^2)$, which makes it impracticable in real processes. In the article we adopted the fast DWMC method to avoid the double looping. In the fast DWMC, we view the AR process as a random sampling process from particle population, and the average agglomeration probability of all particle pairs involved in the AR process can approximate the real average agglomeration probability $\bar{\beta}'_{ij}$ of all possible pairs in the dispersed system. Therefore, the waiting time and the number of agglomeration events in the fast DWMC is estimated as:

$$\Delta t_{agg} = \frac{pN_{st}V}{\sum_{i=1}^{N_{st}} \sum_{j=1,\neq i}^{N_{st}} \beta'_{ij}} = \frac{pN_{st}V}{N_{st}(N_{st}-1)\bar{\beta}'_{ij}} \approx \frac{pVN_{AR}}{(N_{st}-1)\sum_{k=1}^{N_{AR}} \beta'_{ij,k}}, \quad [7]$$

$$N_{agg} = \text{integer}\left[\Delta t \left(N_{st}(N_{st}-1)\sum_{k=1}^{N_{AR}} \beta'_{ij,k}\right) \Big/ (2VN_{AR})\right], \quad [8]$$

where $\beta'_{ij,k}$ is the normalized agglomeration kernel for the kth particle pair in the AR process, N_{AR} is the number of particles pairs involved in the AR process. In order to estimate β'_{max} through only single looping, the weighted majorant kernel $\hat{\beta}'_{ij}$ is introduced here. We define the weighted majorant kernel $\hat{\beta}'_{tr,ij}$ in the transition regime as

$$\hat{\beta}'_{tr,ij} = \frac{\hat{\beta}'_{sf,ij} \cdot \hat{\beta}'_{fr,ij}}{\hat{\beta}'_{sf,ij} + \hat{\beta}'_{fr,ij}}, \quad [9]$$

where the weighted majorant kernel $\hat{\beta}'_{fm,ij}$ in the free-molecular regime is calculated as:

$$\hat{\beta}'_{fm,ij} = 2\sqrt{2}K_{fm}v_j^{1/6}w_j\left[1+\left(\frac{v_{max}}{v_j}\right)^{1/6}+\left(\frac{v_{max}}{v_j}\right)^{2/3}+\left(\frac{v_{min}}{v_j}\right)^{-1/2}\right], \hat{\beta}'_{fm,ij} \geq \beta'_{fm,ij}, \quad [10]$$

and the weighted majorant kernel $\hat{\beta}'_{sf,ij}$ in the slip flow regime as:

$$\hat{\beta}'_{sf,ij} = 2K_{co}w_j\left[\left(\frac{v_{max}}{v_j}\right)^{1/3}+1\right]\left[\left(\frac{v_{min}}{v_j}\right)^{-1/3}+1+2.514\times\left(\frac{\pi}{6}\right)^{1/3}\lambda v_j^{-1/3}\left(\left(\frac{v_{min}}{v_j}\right)^{-2/3}+1\right)\right], \quad \hat{\beta}'_{sf,ij} \geq \beta'_{sf,ij}. \quad [11]$$

Up to now, we can obtain the maximum of weighted majorant kernel ($\hat{\beta}'_{max}$) through only single looping. In such a way, the computational cost of the fast DWMC is reduced to $O(N_{st})$. It is noted that in the fast DWMC method the sample from the AR process is constrained to at least 100 pairs to ensure computational accuracy. Section 3.4 will present the flowchart of the simulation process.

The computational precision and cost of the fast DWMC and normal DWMC are carefully compared and evaluated. The two DWMC methods are applied in Brownian coagulation in the transition regime (initial number concentration $N_0 = 10^{17}$ m^{-3}, initial monodisperse particle diameter $d_0 = 3 \times 10^{-9}$ m, reactor temperature $T = 1473$ K, time period $t = 1000\tau_c$) and agglomeration is only considered in this case. Figure 1 (left) shows that the cost of normal DWMC (with smart bookkeeping technology) is as high as $O(N_{st}^2)$, while for the fast DWMC it is only proportional to N_{st}. Figure 1 (right) shows that the mobility diameter of agglomerates from the normal DWMC and fast DWMC. It is found the fast DWMC can achieve some dozens of speedup ratio. At the same time, the computational accuracy is guaranteed very favorably.

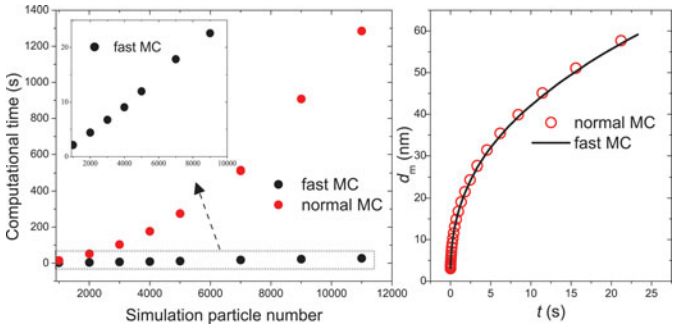

FIG. 1. Comparison between the normal DWMC and fast DWMC: computational time (left); mobility diameter of agglomerates (right). (Color figure available online.)

3.2. Gas Phase Nucleation and Constant-Number Scheme

Within each time step, a nucleation event is implemented until the concentration of precursor is too low to produce enough TiO_2 nuclei, for example, at the end of the aerosol reactor. One simulation particle k is used to represent the new particles generated from the gaseous precursor within Δt and V. It is considered that all of nuclei are spherical primary particles with volume of v_0, diameter of d_0, area of a_0. Their mobility diameter $d_m = d_0$, the diameter of primary particles $d_{pp} = d_0$, the number of primary particles $n_{pp} = 1$. The simulation particle k newly produced has the same internal variables with these real nuclei, and its weight is $w_k = k(t)C_{pre}(t)N_A\Delta tV$. Because nucleation event results in net depletion of gas precursor, the molecular concentration of gas precursor is updated as $C^*_{pre} = C_{pre}(t) - k(t)C_{pre}(t)\Delta t$ after each time step.

It is known that nucleation is dominant in the initial stage of synthesis processes because here the nucleation rate is much faster than the agglomeration rate and sintering rate. Nucleation will continue to increase simulation particle number if no other action is taken. The massive simulation particles will burden computation cost of MC simulation further. The constant number scheme (Lin et al. 2002) is employed in this simulation to recovery the number of simulation particles by contracting the physical volume represented by the simulation while remaining the mass concentration unaffected. In the scheme, when the number of simulation particles exceeds the prespecified upper limit, a particle i selected at random is replaced by the new simulation particle k representing the TiO_2 nuclei. As a result, the volume of computational domain is reduced to:

$$V^* = V\left(1 - \frac{w_i m_i}{\sum_{n=1}^{N_{st}} w_n m_n + w_k m_k}\right). \qquad [12]$$

3.3. Sintering and Monodispersity or Polydispersity of Primary Particles

In the gas-to-particle synthesis processes, sintering and agglomeration are two key mechanisms that affect the size and morphology of particles. Because sintering may change the collision diameter and other interval variables of each simulation particle, the agglomeration rate of each particle pair should be recalculated after each time interval. In order to avoid it, we employ the finite-rate sintering methodology (Rosner and Yu 2001) to uncouple agglomeration and sintering. Within one time interval only agglomerated particles are thought to coalesce from their last agglomeration event to the current time level. This measure thus amounts to that sintering is uncoupled with other events during this time (Δt_{sin}). The measure may introduce some computational error, however will save computational time significantly.

The rate of surface area due to sintering, da/dt, is approximately described by the following equation (Koch and Friedlander 1990):

$$\frac{da}{dt} = -\frac{(a - a_{final})}{\tau_s}. \qquad [13]$$

The monodispersed PP model assumes that agglomerate consists of equal-sized primary particles, which conflicts with experimental measurements. Provided that τ_s is constant over a sufficiently short time step Δt_{sin}, the new surface area of particle i after a sintering event is calculated according to the integrated form of Equation (13):

$$\text{if } a_i > a_{i,final},\ a_i^* = a_i \exp\left(-\frac{\Delta t_{sin}}{\tau_s\left(T, d_{ppi}\right)}\right) + a_{i,final}\left[1 - \exp\left(-\frac{\Delta t_{sin}}{\tau_s\left(T, d_{ppi}\right)}\right)\right]. \qquad [14]$$

Because sintering has no effect on the volume (or mass) of the agglomerate, knowing the new surface area a_i^*, the diameter of primary particles (d^*_{ppi}) after sintering is determined by $6v_i/a_i^*$, its number n^*_{ppi} is $v_i/(\pi {d^*_{ppi}}^2)$. The mobility diameter of the agglomerate (d^*_{mi}) is $({a_i}^*/\pi)^{1/2}$.

Heine and Pratsinis (2007) have proposed the polydisperse PP model to capture internal inhomogeneous structure of agglomerate due to sintering. The polydisperse PP model was integrated into the PB-MC method to describe the detailed evolution of agglomerate and primary particle distribution. It is considered primary particles within agglomerates satisfy polydispersed distribution. That is, an agglomerate is composed of unequally sized PPs, and the size distribution of PPs is classified by specific rule, such as logarithmic rule (150 bins) in this article, in which the smallest PP size is given by the smallest agglomerates ($d_0 = 0.65$ nm), and the maximum PP size is that of the fully coalesced agglomerate. It is assumed that the PPs in a same bin have same size. The polydisperse PP distribution within an aggregate k with volume $v_{agg,k}$ and surface area $a_{agg,k}$ is discretized into $N_{s,pp}$ bins, resulting in the following

conservation relations:

$$v_{\mathrm{agg},k} = \sum_{l=1}^{N_{\mathrm{s,pp}}} (n_{\mathrm{pp},l,k} v_{\mathrm{pp},l,k}); a_{\mathrm{agg},k} = \sum_{l=1}^{N_{\mathrm{s,pp}}} (n_{\mathrm{pp},l,k} a_{\mathrm{pp},l,k}), \quad [15]$$

where the lth bin is characterized by representative volume $v_{\mathrm{pp},l,k}$, area $a_{\mathrm{pp},l,k}$ and number $n_{\mathrm{pp},l,k}$. It is considered that the sintering process has no effect on the scope of PP distribution, however alters the PP number of each bin.

The PBE for the number of primary particles is constructed to obtain the evolution of size distribution of primary particles within agglomerates (Heine and Pratsinis 2007):

$$\frac{\mathrm{d}n_{\mathrm{pp},l,k}}{\mathrm{d}t} = \left(\frac{\mathrm{d}n_{\mathrm{pp},l,k}}{\mathrm{d}t}\right)_{\mathrm{loss}} + \left(\frac{\mathrm{d}n_{\mathrm{pp},l,k}}{\mathrm{d}t}\right)_{\mathrm{gain}} \quad [16]$$

$$\left(\frac{\mathrm{d}n_{\mathrm{pp},l,k}}{\mathrm{d}t}\right)_{\mathrm{gain}} = -\frac{v_{\mathrm{pp},l-1,k}}{v_{\mathrm{pp},l,k}} \left(\frac{\mathrm{d}n_{\mathrm{pp},l-1,k}}{\mathrm{d}t}\right)_{\mathrm{loss}}, \quad [17]$$

$$\left(\frac{\mathrm{d}n_{\mathrm{pp},l,k}}{\mathrm{d}t}\right)_{\mathrm{loss}} = -\frac{n_{\mathrm{pp},l,k}}{\tau_{\mathrm{sin},l}} \cdot \frac{a_{\mathrm{pp},l,k} - a_{\mathrm{final},k}/n^{\mathrm{mono}}_{\mathrm{pp},l,k}}{a_{\mathrm{pp},l,k} - a_{\mathrm{pp},l+1,k} v_{\mathrm{pp},l,k}/v_{\mathrm{pp},l+1,k}}, \quad [18]$$

where $a_{\mathrm{final,k}}$ is the surface area of the sphere after complete coalescence of k, $\tau_{\mathrm{sin,l}}$ is the characteristic sintering time dependent of the lth PP size, $n^{\mathrm{mono}}_{\mathrm{pp},l,k} = v_{\mathrm{agg},k}/v_{\mathrm{pp},l,k}$. Solving the above equations can help us obtain the time evolution of agglomerates and its internal primary particles size distributions. Finally, after a sintering event the number of PPs of bin l within an agglomerate k could be updated as

$$n^{*}_{\mathrm{pp},l,k} = n_{\mathrm{pp},l,k} - (\Delta n_{\mathrm{pp},l,k})_{\mathrm{loss}} + (\Delta n_{\mathrm{pp},l,k})_{\mathrm{gain}}. \quad [19]$$

The surface area and mobility diameter of the agglomerate k is calculated as

$$a^{*}_{\mathrm{agg},k} = \sum_{l=1}^{N_{\mathrm{s,pp}}} \left[\pi n^{*}_{\mathrm{pp},l,k} d^{2}_{\mathrm{pp},l,k}\right]; d^{*}_{\mathrm{m},k} = \sqrt{a^{*}_{\mathrm{agg},k}/\pi}. \quad [20]$$

3.4. Scheme of PBMC Simulation Process

The basic frame of the PB-MC for simultaneous nucleation, agglomeration, and sintering was: within a well-designed time step, the three events were uncoupled and then can be described separately. First, the waiting time between two successive agglomeration events for a simulation particle (Δt_{agg}) was calculated, and the time step Δt was constrained to reasonable time scope to make the uncoupling assumption be reasonable on the whole, then possible agglomeration events, nucleation event, and sintering events were determined in serials. Detailed scheme can be found in the online supplemental information.

4. SIMULATION RESULTS

Nakaso et al. (2001) measured the size distribution of TiO_2 agglomerates and primary particles produced in a plug-flow reactor with an inner diameter of 13 mm and a length of 1.5 m. The reactor is placed in a single controllable electric furnace made of $LaCrO_3$ heating elements. The heating part is between 0.45 m and 0.75 m, which allows the heated gas to cool to room temperature before leaving the reactor. In this experiment, TTIP gas precursor with concentration of 7.679×10^{-7} mol/l enters into the reactor with rate of 2 l/min. A set-point temperature T_{f} is maintained in the middle of reactor. The length-dependent reactor temperature, $T(l)$, is simulated by CFD software utilizing experimental measurements of Seto et al. (1997) as boundary condition. Figure 2 shows experimental measurements by Seto et al. (1997) and CFD simulation results. Gas temperature at axial centerline of reactor is employed in the PB-MC simulations.

The nanoparticles are considered to be fully entrained by gas stream, i.e., the axial velocity $V(l)$ of nanoparticles is assumed same with the axial gas flow velocity at the length l, which is shown in Figure 2.

Simulation results are compared with experimental results and numerical results from the 2-D discrete-sectional (DS) method (Nakaso et al. 2001). Figures 3 (monodisperse PP model for sintering) and 4 (polydisperse PP model for sintering) show the evolution of agglomerate size distribution (ASD) and primary particle size distribution (PPSD) when $T_{\mathrm{f}} = 1200^{\circ}$C. At the forepart of the reactor, the concentration of small size agglomerates and primary particles is high due to nucleation, and tend to decrease due to agglomeration and sintering, respectively. At the outlet, both ASD and PPSD present log-normal distribution. The final products predicted by the MCs have similar geometric mean diameter, standard deviation of agglomerates, and number concentration with the experimental results. With respect to the monodisperse and polydisperse PP models, the simulation results exhibit only a little difference for ASD, while larger difference for PPSD. Both the monodisperse and

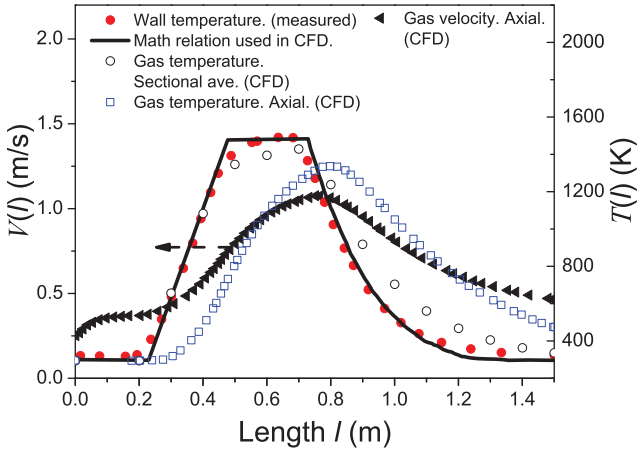

FIG. 2. Temperature profile and gas velocity in the plug-flow aerosol reactor. (Color figure available online.)

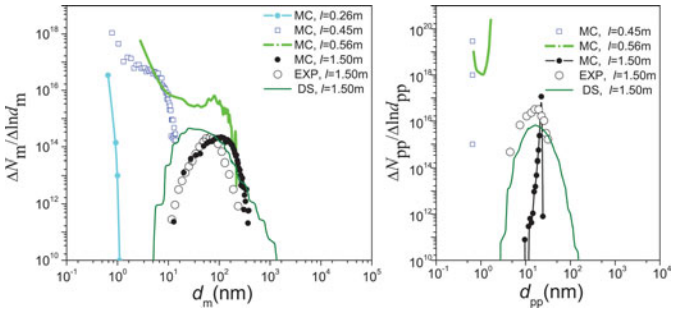

FIG. 3. Monodisperse model results: the change of size distribution of TiO_2 agglomerates (left) and primary particles (right) with l. (Color figure available online.)

polydisperse PP models can predict the mean PP diameter well; however, the monodisperse PP model predicts a larger number concentration of PPs and a smaller geometric standard deviation of PPs. When the polydispersed PP model is used, number concentration, mean diameter, and deviation of PPs agree better with experimental results. Generally, the polydisperse PP model has advantage in numerical precision compared with the monodispersed PP model.

In addition to measurement errors, the discrepancy between PB-MC simulation results and experimental measurements may be due to: (1) the MC does not consider condensation and diffusional wall deposition (Park and Rogak 2003); (2) the inhomogeneity of temperature and concentration profiles is not considered, and the modeled temperature and gas velocity profiles deviate from experimental measurements; (3) the used kernel models (especially τ_s) may not be accurate for the case (Buesser et al. 2011); (4) surface growth will narrow the size distribution in the initial stage, which is not included in this MC (Tsantilis and Pratsinis 2004).

In order to identify the competition between nucleation, agglomeration, and sintering, the characteristic agglomeration rate n_{agg} (the number of particles taking part in agglomeration events in unit time and unit volume, $n_{agg} = N_m(N_m-1)\beta(d_{am,g}, d_{am,g})/2$, $m^{-3}\cdot s^{-1}$, where N_m is the number concentration of agglomerates) and the characteristic nucleation

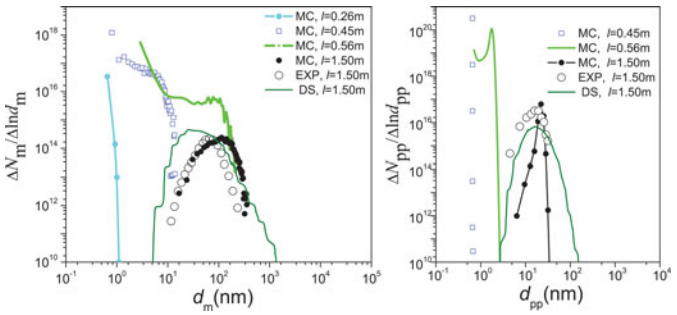

FIG. 4. Polydisperse model results: the change of size distribution of TiO_2 agglomerates (left) and primary particles (right) with l. (Color figure available online.)

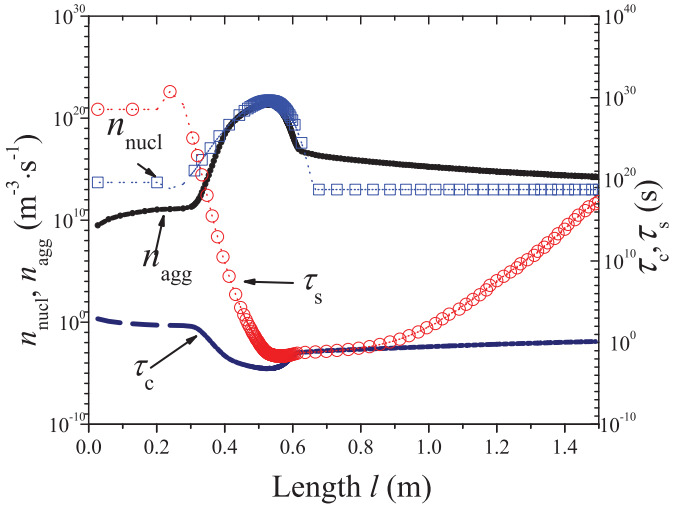

FIG. 5. The trends of n_{nucl} and n_{agg}, τ_c and τ_s with l (1200°C). (Color figure available online.)

rate n_{nucl} (the number of particles produced from gas phase reaction in unit time and unit volume, $n_{nucl} = k(t)C_{pre}(t)N_A$, $m^{-3}\cdot s^{-1}$) are calculated real-timely to identify competition between them. The characteristic agglomeration time ($\tau_c = 1/N_m\beta(d_{am,g},d_{am,g})$, which is defined here as the waiting time of particles both with mobility diameter of $d_{am,g}$), and the characteristic sintering time τ_s of an agglomerate having PP diameter of $d_{pp,g}$ are also compared to measure which dominates the size and morphology of agglomerates (Figure 5). The length-dependent agglomeration number concentration (N_{am}), geometric mean mobility diameter ($d_{am,g}$), geometric standard deviation ($\sigma_{am,g}$), and surface area (a) are shown in Figure 6. Figure 7 presents the evolution of primary particle number concentration (N_{pp}), geometric mean diameter ($d_{pp,g}$), and geometric standard deviation ($\sigma_{pp,g}$).

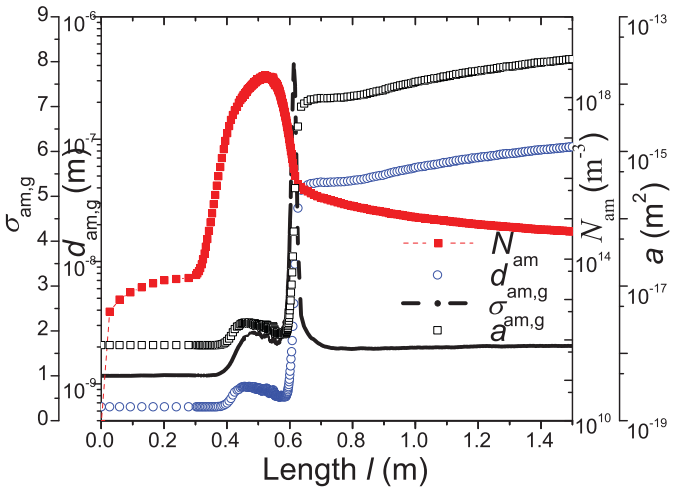

FIG. 6. The moments of size distribution of agglomerates (1200°C). (Color figure available online.)

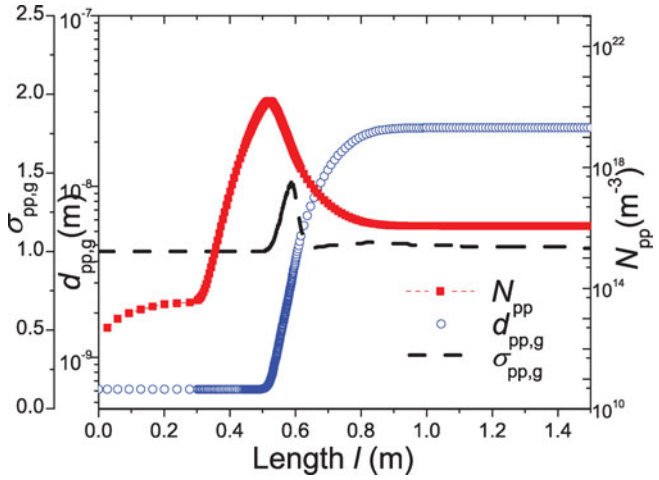

FIG. 7. The moments of size distribution of primary particles (1200°C). (Color figure available online.)

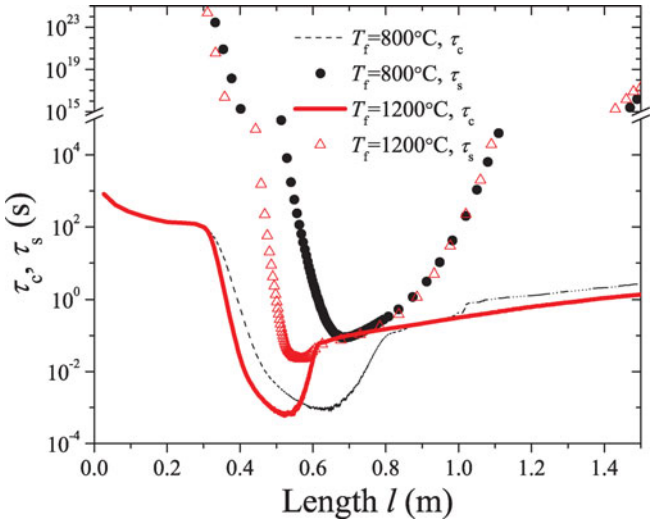

FIG. 9. Trends of characteristic agglomeration time and sintering time at different temperatures (800°C, 1200°C) with l. (Color figure available online.)

As shown in Figure 5, the nucleation is dominant in the initial stage; in the cooling part the agglomeration event prevails over the nucleation; the sintering becomes active in the high-temperature part. It is seen in Figures 5–7 that: (1) in the initial stage, high concentration of precursor results in large number of TiO_2 monomers formed by nucleation. On the other hand, both the reactor temperature and particle number concentration are low, resulting in negligible agglomeration rate and sintering rate. Thus it will lead to large amount of monomers with diameter d_0. $d_{am,g}$ and $d_{pp,g}$ stay stable as d_0, N_{am} and N_{pp} continuously increase; (2) in the high-temperature part, sintering becomes active because of the high temperature and rather small PP diameter. The interaction of nucleation, agglomeration, and sintering will affect the diameter and concentration of particles. Depending on temperature profile, number concentration, and other environmental variables, sintering prevails over agglomeration within some regions, while agglomeration is more dominant within other regions; as a whole, $d_{pp,g}$ and $d_{am,g}$ increase significantly, while N_{am} and N_{pp} start to decrease; (3) in the cooling part, the carrier gas cools down, leading to almost no nucleation and sintering, agglomeration "defeats" other events. Therefore, $d_{am,g}$ continues to increase, N_{am} will decrease, $d_{pp,g}$ and N_{pp} will stay stable.

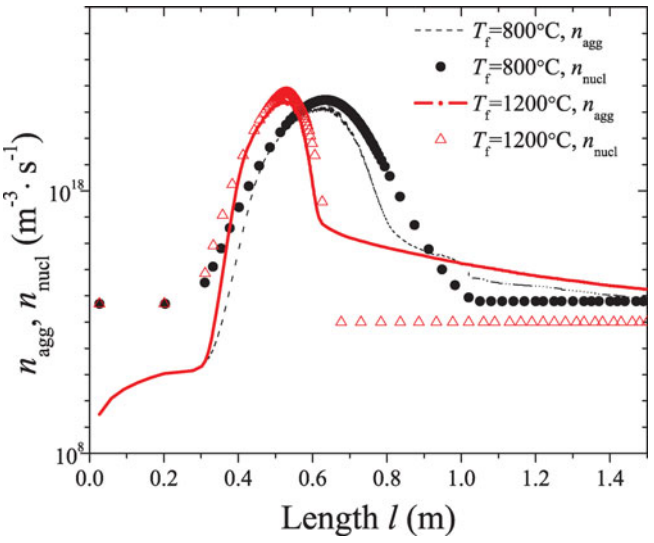

FIG. 8. Trends of characteristic agglomeration rate and nucleation rate at different temperatures (800°C, 1200°C) with l. (Color figure available online.)

Figures 8 and 9 show the mechanism competition at different temperature. Even though Figures 8 and 9 show similar trend at different T_f, temperature history is one of the most important factors in the synthesis process. When T_f increases, nucleation rate is accelerated, resulting in more rapid decrease of precursor concentration. At the same time, agglomeration dominates in advance. With a higher T_f, the dominate region of sintering is enlarged. At $T_f = 800$°C, it is found that sintering almost has no dominate region.

As shown, when T_f increases, particles are formed earlier from gas-phase nucleation process on average, which means that particles will experience longer heated history and higher temperature, resulting in smaller agglomerates and bigger primary particles because of more severe sintering. On the other hand, a higher T_f implies faster velocity of carrier gas, which leads to opposite effect. The interaction of these two aspects can be further studied to identify the effect of temperature on particle diameter and morphology.

5. CONCLUSION

The synthesis process of TiO_2 nanoparticles through thermal decomposition of TTIP in aerosol reactor as an example was simulated via the differently weighted Monte Carlo method. Particular attention in this article was paid to extending DWMC method to simulate simultaneous nucleation, agglomeration, and sintering in real aerosol processes. In order to improve

computational efficiency, we used finite-rate sintering method (Rosner and Yu 2001) to uncouple agglomeration and sintering; on the other hand, we approximated mean agglomeration kernel by the mean of all agglomeration kernels of particle pairs involved in the acceptance–rejection process and estimated the maximum agglomeration kernel from the majorant kernel to avoid double looping over all simulation particles in normal PB-MC method. In order to constrain the drastically increase in simulation particle number due to nucleation events, the idea of constant-number method (Smith and Matsoukas 1998; Lin et al. 2002) was employed to keep simulation particle number constant. In order to capture the structural inhomogeneity of agglomerate particles, we adopted the polydisperse primary particle model (Heine and Pratsinis 2007) for sintering to calculate more realistic primary particle size distribution. The predicted results are satisfactory on the whole. The efficient PB-MC is customized for the gas-to-particle synthesis process and demonstrates its potential in real aerosol processes.

REFERENCES

Bandyopadhyaya, R., Lall, A. A., and Friedlander, S. K. (2004). Aerosol Dynamics and the Synthesis of Fine Solid Particles. *Powder Technol*., 139(3):193–199.

Buesser, B., Grohn, A., and Pratsinis, S. (2011). Sintering Rate and Mechanism of TiO_2 Nanoparticles by Molecular Dynamics. *J. Phys. Chem. C*, 115:11030–11035.

Fox, R. O. (2006). Bivariate Direct Quadrature Method of Moments for Coagulation and Sintering of Particle Populations. *J. Aerosol Sci*., 37(11):1562–1580.

Goodson, M., and Kraft, M. (2004). Simulation of Coalescence and Breakage: An Assessment of Two Stochastic Methods Suitable for Simulating Liquid-Liquid Extraction. *Chem. Eng. Sci*., 59(18):3865–3881.

Heine, M. C., and Pratsinis, S. E. (2007). Polydispersity of Primary Particles in Agglomerates Made by Coagulation and Sintering. *J. Aerosol Sci*., 38(1):17–38.

Hounslow, M. J., Ryall, R. L., and Marshall, V. R. (1988). A Discretized Population Balance for Nucleation, Growth, and Aggregation. *AlChE J*., 34(11):1821–1832.

Kazakov, A., and Frenklach, M. (1998). Dynamic Modeling of Soot Particle Coagulation and Aggregation: Implementation with the Method of Moments and Application to High-Pressure Laminar Premixed Flames. *Combust. Flame*., 114(3–4):484–501.

Kobata, A., Kusakabe, K., and Morooka, S. (1991). Growth and Transformation of TiO_2 Crystallites in Aerosol Reactor. *AlChE J*., 37(3):347–359.

Koch, W., and Friedlander, S. K. (1990). The Effect of Particle Coalescence on the Surface Area of a Coagulating Aerosol. *J. Colloid Interface Sci*., 140(2):419–427.

Kostoglou, M., and Konstandopoulos, A. G. (2001). Evolution of Aggregate Size and Fractal Dimension During Brownian Coagulation. *J. Aerosol Sci*., 32(12):1399–1420.

Kruis, F. E., Kusters, K. A., and Pratsinis, S. E. (1993). Simple Model for the Evolution of the Characteristics of Aggregate Particles Undergoing Coagulation and Sintering. *Aerosol Sci. Technol*., 19:514–526.

Lin, Y., Lee, K., and Matsoukas, T. (2002). Solution of the Population Balance Equation Using Constant-Number Monte Carlo. *Chem. Eng. Sci*., 57(12):2241–2252.

Morgan, N., Wells, C., Kraft, M., and Wagner, W. (2005). Modelling Nanoparticle Dynamics: Coagulation, Sintering, Particle Inception and Surface Growth. *Combust. Theor. Model*., 9(3):449–461.

Muhlenweg, H., Gutsch, A., Schild, A., and Pratsinis, S. E. (2002). Process Simulation of Gas-to-Particle-Synthesis via Population Balances: Investigation of Three Models. *Chem. Eng. Sci*., 57(12):2305–2322.

Nakaso, K., Fujimoto, T., Seto, T., Shimada, M., Okuyama, K., and Lunden, M. M. (2001). Size Distribution Change of Titania Nano-Particle Agglomerates Generated by Gas Phase Reaction, Agglomeration, and Sintering. *Aerosol Sci. Technol*., 35:929–947.

Nakaso, K., Okuyama, K., Shimada, M., and Pratsinis, S. E. (2003). Effect of Reaction Temperature on CVD-Made TiO_2 Primary Particle Diameter. *Chem. Eng. Sci*., 58:3327–3335.

Okuyama, K., Ushio, R., Kousaka, Y., Flagan, R. C., and Seinfeld, J. H. (1990). Particle Generation in a Chemical Vapor Deposition Process with Seed Particles. *AlChE J*., 36(3):409–419.

Otto, E., Fissan, H., Park, S., and Lee, K. (1999). The Log-Normal Size Distribution Theory of Brownian Aerosol Coagulation for the Entire Particle Size Range: Part II—Analytical Solution Using Dahneke's Coagulation Kernel. *J. Aerosol Sci*., 30(1):17–34.

Park, S. H., and Rogak, S. N. (2003). A One-Dimensional Model for Coagulation, Sintering, and Surface Growth of Aerosol Agglomerates. *Aerosol Sci. Technol*., 37(12):947–960.

Patterson, R. I. A., Jasdeep, S., Balthasar, M., Kraft, M., and Wagner, W. (2006). Extending Stochastic Soot Simulation to Higher Pressures. *Combust. Flame*., 145(3):638–642.

Pratsinis, S. E., and Vemury, S. (1996). Particle Formation in Gases: A Review. *Powder Technol*., 88(3):267–273.

Rosner, D. E., and Pyykönen, J. J. (2002). Bivariate Moment Simulation of Coagulating and Sintering Nanoparticles in Flames. *AlChE J*., 48(3):476–491.

Rosner, D. E., and Yu, S. (2001). MC Simulation of Aerosol Aggregation and Simultaneous Spheroidization. *AlChE J*., 47(3):545–561.

Seto, T., Hirota, A., Fujimoto, T., Shimada, M., and Okuyama, K. (1997). Sintering of Polydisperse Nanometer-Sized Agglomerates. *Aerosol Sci. Technol*., 27:422–438.

Seto, T., Shimada, M., and Okuyama, K. (1995). Evaluation of Sintering of Nanometer-Sized Titania Using Aerosol Method. *Aerosol Sci. Technol*., 23(2):183–200.

Shekar, S., Sander, M., Riehl, R. C., Smith, A. J., Braumann, A., and Kraft, M. (2012). Modelling the Flame Synthesis of Silica Nanoparticles from Tetraethoxysilane. *Chem. Eng. Sci*., 70:54–66.

Smith, M., and Matsoukas, T. (1998). Constant-Number Monte Carlo Simulation of Population Balances. *Chem. Eng. Sci*., 53(9):1777–1786.

Tandon, P., and Rosner, D. E. (1999). Monte Carlo Simulation of Particle Aggregation and Simultaneous Restructuring. *J. Colloid Interface Sci*., 213(2): 273–286.

Tsantilis, S., Briesen, H., and Pratsinis, S. E. (2001). Sintering Time for Silica Particle Growth. *Aerosol Sci. Technol*., 34:237–246.

Tsantilis, S., Kammler, H. K., and Pratsinis, S. E. (2002). Population Balance Modeling of Flame Synthesis of Titania Nanoparticles. *Chem. Eng. Sci*., 57(12):2139–2156.

Tsantilis, S., and Pratsinis, S. E. (2004). Narrowing the Size Distribution of Aerosol-Made Titania by Surface Growth and Coagulation. *J. Aerosol Sci*., 35:405–420.

Xiong, Y., and Pratsinis, S. E. (1993). Formation of Agglomerate Particles by Aggregation and Sintering–Part I. A Two-Dimensional Solution of the Population Balance Equation. *J. Aerosol Sci*., 24(3):283–300.

Zhao, H., Kruis, F. E., and Zheng, C. (2009). Reducing Statistical Noise and Extending the Size Spectrum by Applying Weighted Simulation Particles in Monte Carlo Simulation of Coagulation. *Aerosol Sci. Technol*., 43(8): 781–793.

Zhao, H., Kruis, F. E., and Zheng, C. (2010). A Differentially Weighted Monte Carlo Method for Two-Component Coagulation. *J. Comput. Phys*., 229:6931–6945.

Zhao, H., Kruis, F. E., and Zheng, C. (2011). Monte Carlo Simulation for Aggregative Mixing of Nanoparticles in Two-Component Systems. *Ind. Eng. Chem. Res*., 50(18):10652–10664.

Zhao, H., and Zheng, C. (2013). A Population Balance-Monte Carlo Method for Particle Coagulation in Spatially Inhomogeneous Systems. *Comput. Fluids*, 71:196–207.